Central European Journal of Energetic Materials
ISSN 1733-7178; e-ISSN 2353-1843

Cent. Eur. J. Energ. Mater. 2020, *17*(4): 475-491; DOI 10.22211/cejem/131274
Article is available in PDF-format, in colour, at:
http://www.wydawnictwa.ipo.waw.pl/cejem/Vol-17-Number4-2020/CEJEM_01126.pdf

Research paper

Ballistic Analysis of Missile Propulsion in a Perforated Barrel Launcher

Zbigniew Surma, Zbigniew Leciejewski*

Military University of Technology, Faculty of Mechatronics, Armament and Aerospace, 2 gen. S. Kaliskiego Street, 00-908 Warsaw, Poland
** E-mail:* zbigniew.leciejewski@wat.edu.pl

Abstract: This study presents a ballistic analysis of the propulsion of a smart counter-projectile in an active protection system. In order to reduce the pressure of the propellant gases inside the semi-closed barrel of the launcher and to mitigate the effects of the recoil of the launcher, a perforated barrel was chosen. For the system considered, a physical model and a mathematical model of the propulsion of a rocket projectile in a perforated barrel, as well as a computer program, were developed. The gas pressures inside the combustion chamber of the rocket engine and the barrel, as well as the velocity and travel of the missile are the main results from the solution of the presented mathematical model. Based on the resulting calculations, the influence of the holes in the perforated barrel on the operating conditions of the rocket engine, as well as the pressure of propellant gases and the missile velocity inside the barrel were analysed. The use of a perforated barrel caused a significant reduction in the total impulse of the propellant pressure inside the barrel. Based on experimental tests of the barrel launcher-missile assembly, a decrease (about 50%) in the muzzle velocity of the missile was observed. The mathematical model of the interior ballistics presented here allows the missile propulsion, both in a monolithic- as well as a perforated barrel-launcher, to be investigated.

Keywords: mechanics, internal ballistics, rocket propulsion system, perforated barrel

Nomenclature

A Pre-exponential factor in the nonerosive-burning rate law [m/s·Pa^n]
a, b Coefficients of the combustion chamber elaboration of the rocket engine [-]
c_p Isobaric specific heat of the propellant gases [J/kg·K]
c_v Isochoric specific heat of the propellant gases [J/kg·K]
D_0 External diameter of the rocket propellant grains [m]
d Calibre of the barrel [m]
d_0 Internal diameter of the rocket propellant grains [m]
F_e Surface area of the exit nozzle section [m^2]
F_m Surface area of the minimum (critical) nozzle section [m^2]
F_r Surface area of the holes in the barrel through which the propellant gases are released to the surroundings [m^2]
f Pressure function of the burning rate law [m/s]
f_1 Temperature function of the burning rate law [-]
f_p "Force" of the rocket propellant [J/kg]
H Enthalpy of the propellant gases flowing out from the rocket engine combustion chamber into the barrel [J]
H_r Enthalpy of the propellant gases flowing out from the barrel to the surroundings [J]
k Specific heat ratio, $k = c_p/c_v$ [-]
L_0 Length of the rocket propellant grains [m]
l Displacement (distance) of the missile in the barrel [m]
l_m Total distance travelled by the missile along the barrel bore [m]
m Initial mass of the missile [kg]
m_p Rocket propellant mass [kg]
N Number of rocket propellant grains [psc.]
n Pressure exponent in the non-erosive burning rate law [-]
p Pressure of propellant gases in the rocket engine combustion chamber [Pa]
p_b Pressure of propellant gases in the barrel [Pa]
Q Heat delivered to the rocket engine combustion chamber due to burning of the rocket propellant [J]
q_s Heat of combustion of rocket propellant [J/kg]
R Gas constant of the propellant gases [J/kg·K]
r Burning rate of the rocket propellant [m/s]
s_0 Initial burning surface area of the rocket propellant [m^2]
s_b Surface area of the barrel bore cross section [m^2]
T Temperature of the propellant gases in the rocket engine combustion chamber [K]
T_0 Initial temperature [K]

T_b Temperature of the propellant gases in the barrel [K]
t Time [s]
U Internal energy of the propellant gases in the rocket engine combustion chamber [J]
U_b Internal energy of the propellant gases in the barrel [J]
V_0 Initial volume of the barrel (initial volume of the space behind the missile) [m^3]
V_c Geometric volume of the rocket engine combustion chamber [m^3]
v Velocity of the missile [m/s]
v_e Velocity of the propellant gases in the exit nozzle section [m/s]
v_m Maximal velocity of the gases in the rocket engine combustion chamber [m/s]
W Work done by the propellant gases in the barrel related to missile propulsion [J]

α Co-volume of the propellant gases [m^3/kg]
γ Relative mass of the propellant gases which flowed out from the barrel to the surroundings [-]
η Relative mass of the propellant gases which flowed from the rocket engine combustion chamber into the barrel [-]
κ, λ Shape coefficient of the rocket propellant grain [-]
ρ_p Density of the rocket propellant [kg/m^3]
φ Erosive function of the burning rate law [-]
φ_2 Correction factor of the flow of gases from the rocket engine combustion chamber into the barrel [-]
χ Heat loss coefficient [-]
Ψ Relative part of the burned rocket propellant [-]

1 Introduction

Theoretical and experimental research on preventing the penetration of the armour of a combat vehicle by enemy projectiles and missiles is conducted mainly in the following areas:

a) the use of new materials on single and multi-layer armour, which makes it difficult to penetrate, or special shaping of the outer layer of the armour, that changes the final flight path of the projectile [1-4],
b) passive protection, that takes the form of a rigid metal grid (cage) fitted around key sections of the combat vehicle preventing direct (on the surface of the armour) detonation of the shaped charge of the warhead. The grid (cage)

disrupts the shaped charge of the warhead by crushing it or by damaging the fuzing mechanism [5-7],

c) explosive reactive armour (ERA) in the form of metal cassettes (boxes) containing explosive material. This is the most efficient way of protection of armoured vehicles, especially in the case of impact by shaped charge jets (SCJ). After perforation of the ERA cassette casing, the shaped charge jet initiates the explosive material inside. The detonation energy of the explosive, together with the launched casing, cause strong dispersion of the jet, and after penetration of the cassette the armour perforation capability is significantly decreased [8, 9],

d) active protection systems that allow the enemy projectile to be neutralized a short distance from the armoured vehicle [1, 7].

In the present paper, the subject of research and analysis is the propulsion of smart counter-projectiles, which is one of the elements of active protection of combat vehicles against enemy missiles. The ballistics of propulsion systems (such as that shown in Figure 1) is the topic of interest in the paper. The analysed propulsion systems consist of two basic assemblies:

(1) a semi-closed barrel launcher, and
(2) a missile installed with a solid propellant rocket engine.

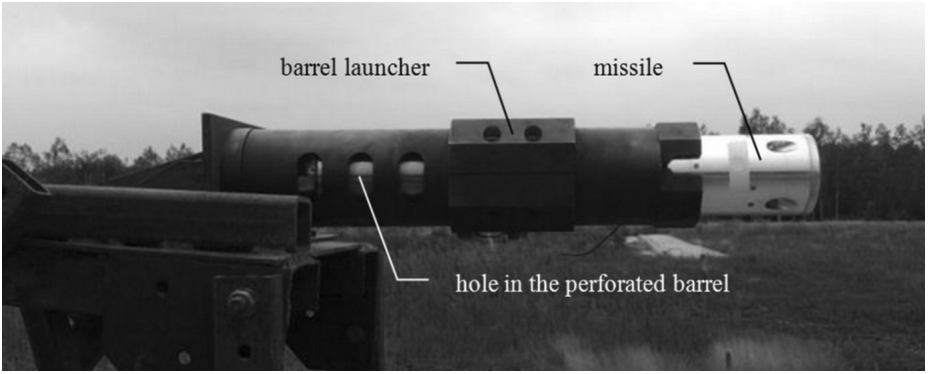

Figure 1. Research stand: launcher with perforated barrel loaded with a missile

Taking into account the tactical requirements, among other aspects, fighting the enemy missile within a short range (10 to 15 m from the protected vehicle), the maximum velocity of a missile ~180 m/s and the limited time from detection to destruction of the enemy missile, a few studies [10-12] have been carried out on the ballistics of the presented rocket propulsion systems.

These studies focused on investigating the solid propellant rocket engine,

the type of rocket propellant, as well as the ignition method of the rocket propellant. In one considered arrangement, the initial stage of missile propulsion in the barrel is influenced by the thrust of the rocket engine (which is installed in the missile) and the pressure of the propellant gases present in the space behind the missile in the barrel. The propellant gases occupy the space behind the missile as they exit the combustion chamber of the rocket engine. One of the ways to significantly reduce the pressure of the propellant gases present in the space behind the missile is to use a perforated barrel, where some of the propellant gases are released to the surrounding space through the holes when the missile is fired from the launcher (Figure 2).

However, it is crucial to ensure that the tactical requirements of the barrel launcher-missile assembly is fulfilled, that is, to fight an enemy missile at a predetermined distance from the protected vehicle.

Figure 2. Propellant gases flowing from the barrel through the holes during firing

2 Materials and Methods

2.1 Simulations

The principles of designing solid propellant rocket engines and modelling their operation in a classic barrel launcher (open on both sides) with the outflow of gases into the unlimited space are known [13-17]. In the present study, a physical model and a mathematical model of the propulsion of a missile in a semi-closed perforated barrel were developed. The equations of the mathematical model were formulated based on the thermodynamic approach, with the focus on the operation of gun propellant systems. Numerical simulations were then carried out

to examine the effects on the missile motion of gas outflow from the holes along the lateral surface of the barrel. The pressure of the propellant gases, the velocity of the missile as it moves along in the barrel bore, and the characteristics of the rocket engine operation, were obtained by numerically solving the governing equations of the mathematical model. The simulation results were validated by comparing them with those obtained from experimental field tests.

2.2 Physical model

When launching a missile, the primary force that drives the motion of the missile is the thrust of the rocket engine. However, in the launcher considered here, the barrel inlet is closed with a breech and the propellant gases formed during the operation of the rocket engine flow into the space behind the missile. The high-pressure propellant gases acting on the bottom of the missile increase its velocity, which drives the missile forward. However, these high-pressure gases also result in a backward movement of the launcher as the missile is launched. One of the ways to reduce the pressure of the propellant gases is to use a perforated barrel (Figure 1).

The perforated barrel was constructed with three oval holes (slots) on each side. The propellant gases will be released to the surroundings from the space behind the projectile through these holes in the barrel. A physical model of the barrel launcher-missile assembly was built in order to perform the ballistic tests, as shown in Figure 3.

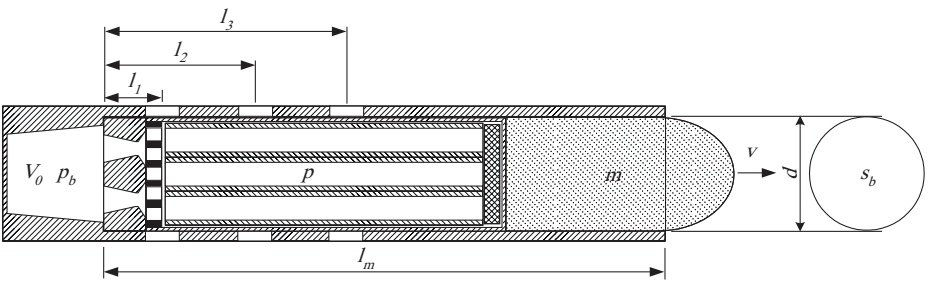

Figure 3. Physical model of the barrel launcher-missile assembly

A set of phenomena were considered for the ballistic tests, beginning from the time when the combustion of the solid propellant was initialised, to the time when the missile (m) exited the barrel. Within this period, the missile is driven by the thrust force generated by the rocket engine. The pressure force (p_b) of the propellant gases will increase the velocity (v) of the missile, covering a distance (l) which is equal to the length of the barrel bore (l_m). The holes open consecutively

at a distance (l_1, l_2 and l_3) as the missile moves along the barrel. The propellant gases are released to the surroundings when these holes are opened.

2.3 Mathematical model

The mathematical model was developed to describe the phenomena that take place in the combustion chamber of the rocket engine and barrel of the launcher. These phenomena comprise the combustion of the rocket propellant, the outflow of gases with time-varying pressure from the combustion chamber of the rocket engine into the space behind the missile in the barrel, the part of the propellant gases flowing out from the space behind the missile in the barrel to the surroundings through the holes, and motion of the missile along the barrel bore. It should be noted that the mathematical model was developed separately for the phenomena in the combustion chamber of the rocket engine and the phenomena in the barrel of the launcher.

The following assumptions were made in formulating the equations of the mathematical model in order to simulate the operation of the barrel launcher-missile assembly [13, 14]:

- Ignition and combustion of the propellant grains proceed according to the geometric model.
- The thermodynamic characteristics of the propellant gases (*e.g.* specific heat ratio and gas constant) are constant throughout the process.
- The propellant gases flowing out from the combustion chamber of the rocket engine into the barrel and from the barrel to the surroundings is an adiabatic, quasi-steady, and one-dimensional process.
- The heat losses in the combustion chamber are accounted for in the analysis based on the reduction in the heat of combustion. This is done by using a heat loss coefficient that is a function of the relative mass of the burned propellant grains.
- The heat losses in the barrel (specifically in the space behind the missile) are neglected from the analysis.

A mathematical-physical model of the solid propellant rocket motor operation can be built using internal ballistic laws and by considering the individual characteristics of the propellant charge, combustion chamber and nozzle dimensions [18-22].

In this study, the governing equations used to describe the phenomena that take place in the solid propellant rocket engine were derived from the energy balance equation based on the first law of thermodynamics. The energy balance of the propellant gases in the combustion chamber of the rocket engine is given by:

$$dU = dQ - dH \tag{1}$$

Noting that:

$$dU = d(c_v m_p(\psi - \eta)T) = c_v m_p(T(d\psi - d\eta) + (\psi - \eta)dT)$$
$$dQ = d(\chi q_s m_p \psi) = \chi q_s m_p d\psi + q_s m_p \psi d\chi$$
$$dH = c_p m_p T d\eta$$

Substituting the definitions for dU, dQ and dH into Equation 1 yields:

$$\frac{dRT}{dt} = \frac{(k-1)q_s\left(\chi\frac{d\psi}{dt} + \psi\frac{d\chi}{dt}\right) - RT\left(\frac{d\psi}{dt} + (k-1)\frac{d\eta}{dt}\right)}{\psi - \eta} \tag{1a}$$

The equation of state for the propellant gases in the combustion chamber of the rocket engine is given by:

$$p = \frac{m_p(\psi - \eta)RT}{V_c - \frac{m_p}{\rho_p}(1-\psi) - \alpha m_p(\psi - \eta)} \tag{2}$$

The rate of the relative mass of the gas generated by combustion of the propellant (gas inflow) can be written as [14]:

$$\frac{d\psi}{dt} = \frac{\rho_p}{m_p} \cdot s_0 \sqrt{1 + 4\frac{\lambda}{\kappa}\psi} \cdot r(p, T_0, v_m) \tag{3}$$

The burning rate law is given by:

$$r(p,T_0,v_m) = f(p) \cdot f_1(T_0) \cdot \varphi(v_m) \tag{4}$$

where $f(p)$, $f_1(T_0)$ and $\varphi(v_m)$ represent the pressure function, the temperature function, and the erosive function, respectively.

The rate of the relative mass of propellant gases flowing out from the combustion chamber of the rocket engine (gas outflow) into the barrel, taking into account the time-varying pressure of the gases in the space behind the missile, can be written as [23]:

$$\frac{d\eta}{dt} = \frac{\varphi_2 F_m}{m_p}\left(\frac{2}{k+1}\right)^{\frac{1}{k-1}}\sqrt{\frac{2k}{k+1}}\frac{p}{\sqrt{RT}} \qquad \text{where} \quad p_b \le p\left(\frac{2}{k+1}\right)^{\frac{k}{k-1}} \tag{5}$$

$$\frac{d\eta}{dt} = \frac{\varphi_2 F_m}{m_p}\sqrt{\frac{2k}{k-1}\left[\left(\frac{p_b}{p}\right)^{\frac{2}{k}} - \left(\frac{p_b}{p}\right)^{\frac{k+1}{k}}\right]}\frac{p}{\sqrt{RT}} \quad \text{where} \quad p_b > p\left(\frac{2}{k+1}\right)^{\frac{k}{k-1}} \tag{5a}$$

The heat loss coefficient χ and the heat loss derivative $d\chi/dt$ can be expressed as [14, 21]:

$$\chi = 1 - \frac{a}{1+b\psi} \;\ldots\; \frac{d\chi}{dt} = \frac{ab}{(1+b\psi)^2}\frac{d\psi}{dt} \tag{6}$$

Likewise, the governing equations used to describe the phenomena that take place in the barrel of the launcher are derived from the energy balance equation based on the first law of thermodynamics. The energy balance of the propellant gases in the barrel is given by:

$$dU_b = dH - dH_r - dW \tag{7}$$

Noting that:

$$dU_b = d(c_v m_p(\eta - \gamma)T_b)$$
$$dH = c_p m_p T d\eta$$
$$dH_r = c_p m_p T_b d\gamma$$
$$dW = (s_b - F_e)p_b dl$$

Substituting the definitions for dU_b, dH, dH_r and dW into Equation 7 yields:

$$\frac{d\left(m_p(\eta-\gamma)RT_b\right)}{dt} = m_p k\left(RT\frac{d\eta}{dt} - RT_b\frac{d\gamma}{dt}\right) - (k-1)(s_b - F_e)p_b v \tag{7a}$$

The equation of state for the propellant gases in the barrel is given by:

$$p_b = \frac{m_p(\eta-\gamma)RT_b}{V_0 + s_b l - \alpha m_p(\eta-\gamma)} \tag{8}$$

The rate of the relative mass rate of propellant gases flowing out from the barrel (gas outflow) to the surroundings can be written as:

$$\frac{d\gamma}{dt} = \frac{F_r}{m_p}\left(\frac{2}{k+1}\right)^{\frac{1}{k-1}}\sqrt{\frac{2k}{k+1}}\frac{p_b}{\sqrt{RT_b}} \tag{9}$$

The equation of missile motion can be expressed as:

$$\frac{dv}{dt} = \frac{m_p\dfrac{d\eta}{dt}v_e + s_b p_b}{m - \eta m_p} \quad \text{where} \quad v_e = \sqrt{\frac{2k}{k-1}RT\left(1-\left(\frac{p_b}{p}\right)^{\frac{k-1}{k}}\right)} \tag{10}$$

The missile velocity can be written as:

$$\frac{dl}{dt} = v \tag{11}$$

The following initial conditions were used for the numerical simulations:

- $t = 0$,
- $\Psi = 0.001$,
- $\eta = \gamma = 0$,
- $\chi = \chi(\Psi)$,
- $l = v = 0$,
- $RT = f_p$,
- $m_p(\eta - \gamma)RT_b = 0$.

3 Results of Numerical Simulations and Experimental Validation

A computer program was developed in order to solve the governing equations of the mathematical model of the launcher-missile assembly with a perforated barrel. For a solution of ordinary first-order differential equations, a fourth-order Runge-Kutta numerical method was applied. Based on work pertaining to the erosive burning stability of a rocket engine [24-27], the effect of gas flow velocity on the propellant burning rate was neglected from the analysis, and it was assumed that the erosive function is $\varphi(v_m) = 1$ for the burning rate law given by Equation 4. The numerical simulations were performed for ambient temperature ($T_0 = 293$ K) and it was assumed that the temperature function is $f_1(T_0) = 1$. Finally, the burning

rate law (Equation 4) is given by power law form and $r(p) = Ap^n$.

The characteristics of the solid propellant, rocket engine, missile and barrel of the launcher used in the numerical simulations are presented in Table 1.

Table 1. Input data used in the numerical simulations [10, 12]

Solid rocket propellant		Rocket engine, missile and barrel	
D_0 [m]	$22.8 \cdot 10^{-3}$	a [-]	0.16
d_0 [m]	$16.4 \cdot 10^{-3}$	N [pcs.]	7
L_0 [m]	$170 \cdot 10^{-3}$	b [-]	2
m_p [kg]	0.380	V_c [m^3]	$0.700 \cdot 10^{-3}$
ρ_p [kg/m^3]	1620	F_m [m^2]	$491 \cdot 10^{-6}$
q_s [J/kg]	$4.5 \cdot 10^6$	F_e [m^2]	$1963 \cdot 10^{-6}$
f_p [J/kg]	$0.9476 \cdot 10^6$	φ_2 [-]	0.9
A [m/s·Pa^n]	$3.30 \cdot 10^{-6}$	m [kg]	5.5
n [-]	0.526	d [m]	$81 \cdot 10^{-3}$
k [-]	1.25	V_0 [m^3]	$0.226 \cdot 10^{-3}$
κ [-]	1.019	l_m [m]	0.406
λ [-]	–0.018		

Investigation of the influence of the surface area F_r on the missile muzzle velocity and the total impulse of the pressure of the propellant gases inside the barrel were initially performed. Simulations were made for the total surface of holes (F_r): 15, 30, 45, 60 and 75 cm^2. Six identical holes (three on each side of the barrel) are opened consecutively as the missile moves along in the barrel of the launcher: l_1 = 22.5 mm, l_2 = 72.5 mm, l_3 = 122.5 mm (Figure 3).

For comparison purposes, numerical simulations were also carried out for a launcher-missile assembly with a monolithic barrel ($F_r = 0$). The simulation results obtained for launchers with different surface areas of holes are shown in Figure 4.

The use of a launcher with a perforated barrel reduces, within the considered range of the surface area of holes, the muzzle velocity of the missile and the total impulse of the pressure of propellant gases inside the barrel by about 55% and 70%, respectively. It is particularly advantageous to reduce the impulse of the pressure causing the undesirable recoil of the barrel launcher.

Subsequently, considering the results obtained from the calculations and the tactical requirements for a Polish smart system, a perforated barrel was constructed with three oval holes (slots) on each side, where each hole has the same dimensions of 20×45 mm. The total surface area of the holes from which the propellant gases will be released from the space behind the missile

to the surroundings was determined to be 48.84 cm^2. The characteristics of the holes in the experimental perforated barrel are listed in Table 2.

Table 2. Characteristics of the holes in the perforated barrel of the launcher

l_i [mm]	22.5	72.5	122.5
F_r [cm^2]	16.28	32.56	48.84

The simulation results obtained for the launcher-missile assembly with a monolithic barrel and a perforated barrel are shown in Figures 5-7. The simulation results were validated by comparing them with those obtained from the experimental field tests. The missile velocity was determined from the images captured using a Phantom v12.1 high-speed camera (Vision Research Inc., USA) and the data were analysed using TEMA Motion v. 3.5 analysis software [28].

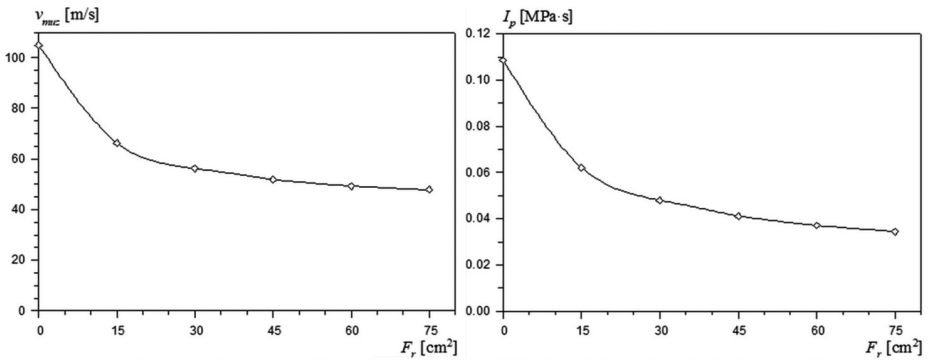

(a) (b)

Figure 4. Variations of the muzzle velocity v_{muz} (a) and the total impulse I_p (b) of the pressure of the propellant gases inside the barrel as a function of surface area F_r of the holes

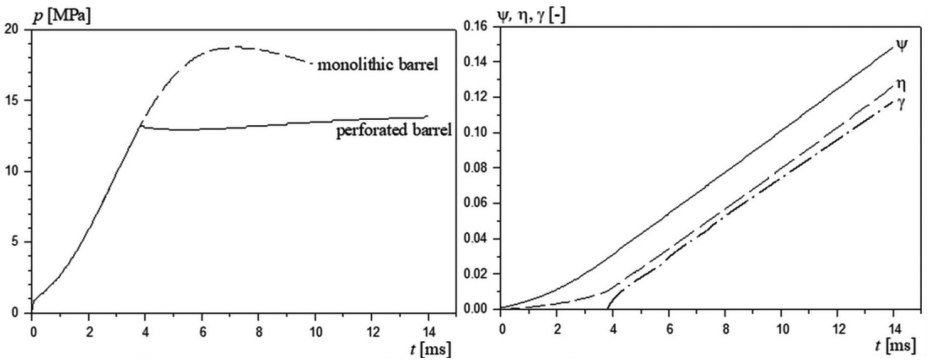

Figure 5. Variations (as a function of time t) of the pressure p in the combustion chamber of the rocket engine and the relative mass of: the burned propellant Ψ, the propellant gases flowing out from the combustion chamber of the rocket engine into the barrel η, and the propellant gases flowing out from the barrel γ, for the launcher-missile assembly with a perforated barrel

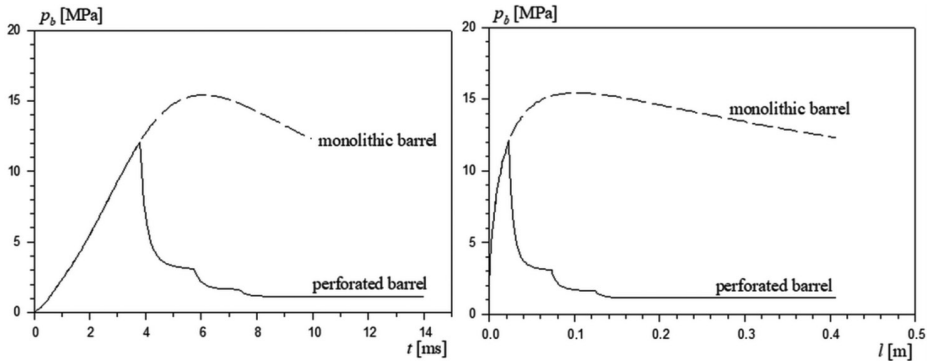

(a) (b)

Figure 6. Variations of the pressure p_b in the barrel as a function of (a) time t and (b) distance l travelled by the missile in the barrel bore

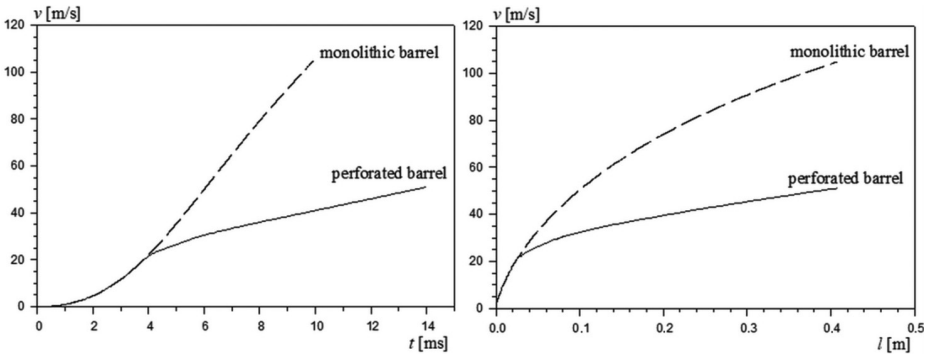

(a) (b)

Figure 7. Variations of the missile velocity v as a function of (a) time t and (b) distance l travelled by the missile in the barrel bore

Figure 8 shows the comparison between the missile velocity obtained from the numerical simulations and the experimental field tests for the barrel launcher-missile assembly with different types of barrel (monolithic and perforated). It can be seen from Figure 8(b) that two phases of phenomena are visible in the launcher-missile assembly with the perforated barrel. These phases are separated by an inflection point, indicating the time when the propellant gases begin to flow out from the holes of the perforated barrel to the surroundings. The phenomena that take place in the barrel launcher-missile assembly are slightly longer during the experimental field tests owing to the slower increase in the initial velocity of the missile.

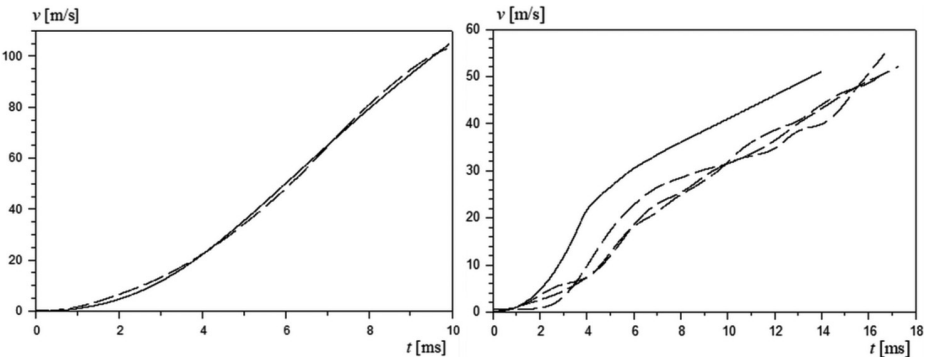

(a) (b)

Figure 8. Variations of the missile velocity v as a function of time t for the barrel launcher-missile assembly with (a) monolithic barrel and (b) perforated barrel; the solid lines and dashed lines indicate the results obtained from simulations and experiments, respectively

In general, there is good agreement between the simulation and experimental results, since the difference between the muzzle velocity determined from the experiments and that obtained from the simulations is less than 5%.

4 Conclusions

The following conclusions can be drawn based on the results obtained from the numerical simulations and the experimental field tests in this study:

- A mathematical model of missile propulsion in a semi-closed perforated barrel was developed. A computer program was also developed in order to simulate the phenomena that occur simultaneously during the operation of the barrel launcher-missile assembly:
  (1) operation of the rocket engine,
  (2) the motion of the missile along the barrel bore of the launcher, and
  (3) the flow of the propellant gases from the barrel to the surroundings
- It is possible to significantly reduce the pressure (total impulse) of the propellant gases inside the barrel (and thus minimise recoil) by using a perforated barrel.
- The use of a launcher with a perforated barrel reduces, within the considered (investigated) system configuration, the total impulse of the pressure of propellant gases inside the barrel and the muzzle velocity of the missile by about 60% and 50%, respectively.
- There is good agreement for the velocity of the missile moving in the barrel bore between the numerical simulations and the experimental field tests, which indicates the physical correctness and practical suitability of the presented mathematical model.
- The mathematical model developed in this study can be used beyond the range of test conditions presented in this paper because the computer program can be used to simulate the operation of the rocket engine until the propellant charge is completely burned out.

Funding

This work was supported by the Polish National Centre for Research and Development [Grant no.: DOBR-BIO4/031/13249/2013].

References

[1] Madhu, V.; Balakrishna Bhat, T. Armour Protection and Affordable Protection for Futuristic Combat Vehicles. *Def. Sci. J.* **2011**, *61*(4): 394-402.

[2] Flores-Johnson, A.E.; Saleh, M.; Edwards, L. Ballistic Performance of Multi-layered Metallic Plates Impacted by a 7.62-mm APM2 Projectile. *Int. J. Impact Eng.* **2011**, *38*(12): 1022-1032.

[3] Kędzierski, P.; Morka, A.; Sławiński, G.; Niezgoda, T. Optimization of Two-component Armour. *Bull. Pol. Ac.: Tech*. **2015**, *63*(1): 173-179.

[4] Stanisławek, S.; Morka, A.; Niezgoda, T. Pyramidal Ceramic Armour Ability to Defeat Projectile Threat by Changing Its Trajectory. *Bull. Pol. Ac.: Tech*. **2015**, *63*(4): 843-849.

[5] Panowicz, R.; Niezgoda, T. Experimental Studies on Protection Systems of Military Vehicles against RPG Type Missiles. *Solid State Phenom.* **2016**, *240*: 244-249.

[6] Niezgoda, T.; Panowicz, R.; Sybilski, K.; Barnat, W. Numerical Analysis of a Shell with a Main Charge Warhead Stroke into a Bar Armour with Square Section. *J. KONES Powertrain and Transport* **2010**, *17*(3): 327-332.

[7] Dean, E.S. Active and Reactive Vehicle Protection Systems. *European Security & Defence* **2019**, https://euro-sd.com/2019/05/articles/13297/active-and-reactive-vehicle-protection-systems/ [accessed on 2020-10-18].

[8] Wiśniewski, A. Research of ERAWA-1 and ERAWA-2 Reactive Cassettes. *Problemy Mechatroniki. Uzbrojenie, Lotnictwo, Inżynieria Bezpieczeństwa (Problems of Mechatronics. Armament, Aviation, Safety Engineering)* **2019**, *10*(3): 9-18.

[9] Liden, E.; Helte, A.; Lundgren, J. Influence of Intermediate Layers in Reactive Armours Modules on the Protection Capability. *Proc. 31st Int. Symp. Ballistics,* Hyderabad, India, **2019**, vol. 2, 1260-1271.

[10] Kupidura, P.; Leciejewski, Z.; Surma, Z.; Zahor, M. Theoretical and Experimental Investigations on Rocket Propulsion of Counterprojectile of Active Protection System. *Proc. 29th Int. Symp. Ballistics,* Edinburgh, Scotland, **2016**, vol. 1, 681-691.

[11] Surma, Z.; Zahor, M.; Kupidura, P.; Leciejewski, Z. Preliminary Studies of a Propellant System for the Counterprojectile of an Active Protection System. *Problemy Mechatroniki. Uzbrojenie, Lotnictwo, Inżynieria Bezpieczeństwa (Problems of Mechatronics. Armament, Aviation, Safety Engineering)* **2017**, *8*(2): 33-42.

[12] Surma, Z.; Leciejewski, Z.; Dzik A.; Białek, M. Theoretical and Experimental Investigations on Rocket Propulsion System of Projectile Intended for Vehicle Active Protection System. *Mater. Wysokoenerg. (High Energ. Mater.)* **2017**, *7*: 44-52.

[13] Carlucci E.D.; Jacobson S.S. *Ballistics: Theory and Design of Guns and Ammunition.* 2nd ed., CRC Press Taylor & Francis Group, Boca Raton, **2014**.

[14] Serebryakov, M.E. *Internal Ballistics of Gun Systems and Solid Rockets.* (in Russian) Oborongiz, Moscow, **1962**.

[15] Mahjub, A.; Mazlan, N.M.; Abdullah, M.Z.; Azam, Q. Design Optimization of Solid Rocket Propulsion: a Survey of Recent Advancements. *J. Spacecr. Rockets* **2020**, *57*(1): 3-11.
[16] Zeping, W.; Donghui, W.; Weihua, Z.; Około, P.; Yang, F. Solid-rocket-motor Performance-Matching Design Framework. *J. Spacecr. Rockets* **2017**, *54*(3): 698-707.
[17] Kuentzmann, P. *Introduction to Solid Rocket Propulsion*. NATO Report No. RTO-EN-023, **2004**, 1-16.
[18] Villanueva, F.M.; He, L.S.; Xu, D.J. Solid Rocket Motor Design Optimization using Genetic Algorithm. *Adv. Mater. Res.* **2014**, *905*: 502-506.
[19] Terzic, J.; Zecevic, B.; Baskarad, M.; Catovic, A.; Serdarevic-Kadic, S. Prediction of Internal Ballistic Parameters of Solid Propellant Rocket Motors. *Problemy Mechatroniki. Uzbrojenie, Lotnictwo, Inżynieria Bezpieczeństwa (Problems of Mechatronics. Armament, Aviation, Safety Engineering)* **2011**, *2*(4): 7-26.
[20] Tola, C.; Nikbay, M. Internal Ballistic Modeling of a Solid Rocket Motor by Analytical Burnback Analysis. *J. Spacecr. Rockets* **2018**, *56*(2): 1-19.
[21] Zygmunt, B.; Surma, Z.; Leciejewski, Z.; Motyl, K.; Rasztabiga, T. Modelling and Verification of Solid Propellant Rocket Motor Operation. *Cent. Eur. J. Energ. Mater.* **2016**, *13*(4): 944-956.
[22] Cavallini, E.; Favini, B.; Giacinto, M.D.; Serraglia, F. Internal Ballistics Simulation of a NAWC Tactical SRM. *J. Appl. Mech.* **2011**, *78*(5): 051018 (8 pages).
[23] Hill, R.; McLeod, L. Analysis of Inter-chamber Energy and Mass Transport in High-Low Pressure Gun Systems. *Proc. 28th Int. Symp. Ballistics,* Atlanta, USA, **2014**, vol. 1, 459-470.
[24] Razdan, M.K.; Kuo, K.K. Erosive Burning of Solid Propellant. In: *Fundamentals of Solid-Propellant Combustion. Progress in Astronautics and Aeronautics*. (Kuo, K.K.; Summerfield, M., Eds.) American Institute of Aeronautics and Astronautics, Washington. **1984**, vol. 90, pp. 515-598.
[25] Abdelaziz, A.; Guozhu, L.; Elsayed, A. Parameters Affecting the Erosive Burning of Solid Rocket Motor. *MATEC Web Conf.* **2018**, *153*: 03001.
[26] Ma, Y.; Bao, F.; Hui, W.; Liu Y.; Wei, R. An Approach to Analysing Erosive Characteristics of Two-channel Combustion Chambers. *Int. J. Aerosp. Eng.* **2019**, DOI: 10.1155/2019/2974537.
[27] Safta, D.; Ion, I. Towards the Effects of Initial Grain Temperature and Erosive Burning on the Solid Propellant Combustion. *INCAS Bull.* **2018**, *10*(4): 125-140.
[28] *Image Systems Motion Analysis, TEMA Motion.* from http://www.imagesystems.se/tema/, [accessed on 2019-08-03].

Received: February 27, 2020
Revised: December 8, 2020
First published online: December 18, 2020